Journal of the Korean Physical Society, Vol. 44, No. 6, June 2004, pp. 1412∼1416

# First-Order Analysis of Thin-Plate Deformable Mirrors

Jun Ho Lee*
*Satellite Technology Research Center, Korea Advanced Institute of Science and Technology, Daejeon 305-701*

Tae-Kyoung Uhm† and Sung-Kie Youn‡
*Department of Mechanical Engineering, Korea Advanced Institute of Science and Technology, Daejeon 305-701*

(Rceived 4 February 2004)

Continuous thin-plate deformable mirrors with discrete actuators are widely used as adaptive mirrors. The performance of a thin-plate deformable mirror can be characterized by the influence functions and the layout of the actuators. This paper first derives equations that model the influence functions of thin-plate deformable mirrors based on an analytic calculation and a finite- element analysis; then, it presents a performance analysis for the cases of triangular, rectangular, and hexagonal patterned-actuators. The results from this study may be used for first-order design and analysis of thin-plate deformable mirrors.

PACS numbers: 42
Keywords: Adaptive optics, Deformable mirror, Opto-mechanics

## I. INTRODUCTION

Adaptive optics (AO) systems remove the wavefront distortion introduced by the earth's atmosphere (or other turbulent medium) by means of an optical component(s) or wavefront corrector(s) introducing a controllable counter wavefront distortion which both spatially and temporally follows the wavefront distortion of the atmosphere [1,2]. Among several wavefront correctors (Fig. 1), the continuous thin-plate mirror with discrete actuators is widely used as an adaptive mirror [3].

A thin-continuous deformable mirror changes its surface shape by pushing or pulling discrete actuators, and the number of producible modes or shapes generally increases with the number of actuators. However, if system speed is to be improved and development, and maintenance costs reduced, a minimum number of actuators should be located at optimal positions. Therefore, as a prerequisite for finding the optimal number of actuators and their layout, it is necessary to investigate how the performance of a deformable mirror varies with the number of actuators, and their layout and with the influence functions of actuators. The performance of a thin-plate deformable mirror can be characterized by the influence functions and the layout of the actuators. The shape of the influence function is controlled by the mechanical properties of the mirror and the actuator and by the boundary conditions. The main mechanical properties of concern are the ratio of the faceplate bending stiffness to the actuator bending and axial stiffnesses and the size and the shape of the pusher pad that transfers the actuator force to the faceplate. The major boundary conditions are the relative distances and the coupling effect of neighboring actuators and edges.

Previous studies have been performed to set up mathematical models of the influence functions [4-8]. Hudgin used tip/tilt, Gaussian and pyramidal influence functions in his study [4] and Taranenko *et al.* derived the influence functions of metal mirrors as exponential functions [5]. However, the previous studies did not include the coupling effect between actuators; furthermore, it is necessary to construct influence function models incorporating analytic calculations and finite-element analyses, which can be efficiently used in the first-order design of thin-plate deformable mirrors.

This paper first derives equations that model the influence functions based on analytic calculations and a finite-element (FE) analysis. Then deformable mirrors with triangular, rectangular, and hexagonal actuator patterns are analyzed. Based on the analyses, the dependence of the performance on design parameters, such as the coupling coefficient between actuators, is derived and base-

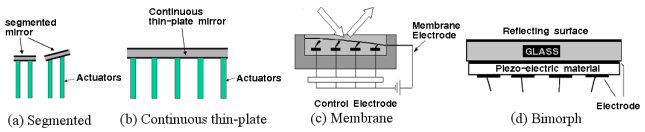


Fig. 1. AO deformable mirrors.

*E-mail: jhl@satrec.kaist.ac.kr
†E-mail: taerii@kaist.ac.kr
‡E-mail: skyoun@sorak.kaist.ac.kr

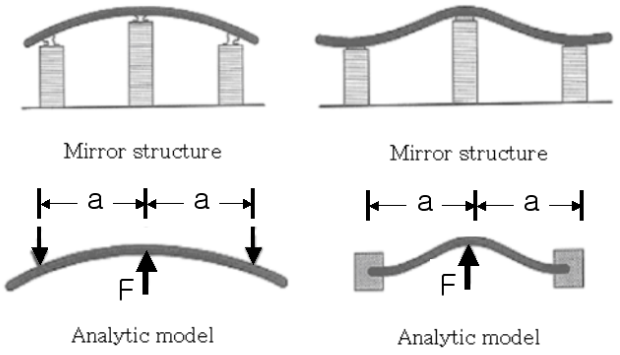


Fig. 2. Deformable mirror models used by Hardy in his analytic derivation [2].

line values of the design parameters for optimal performance are proposed.

## II. ESTIMATIES OF THE INFLUENCE FUNCTIONS

### 1. Influence Functions of Ideal Deformable Mirrors

Hardy [3] calculated, based on simple beam deflection theory, the influence functions or the deflections of a mirror for the cases of infinitely stiff faceplates and infinitely stiff actuators as given in Eqs. (1) and (2), respectively:

$$y_1 = \frac{a^3 F}{6EI}\left[\frac{1}{2}\left(\frac{x}{a}\right)^3 - \frac{3}{2}\left(\frac{x}{a}\right)^2 + 1\right], \tag{1}$$

$$y_2 = \frac{a^3 F}{24EI}\left[2\left(\frac{x}{a}\right)^3 - 3\left(\frac{x}{a}\right)^2 + 1\right], \tag{2}$$

where $y_1$ is the deflection of a deformable mirror with an infinitely stiff faceplate, $y_2$ the deflection of a deformable mirror with an infinitely stiff actuator, $x$ the (positive) distance from the center of the actuator, $F$ the force applied by the center actuator, $a$ the actuator spacing distance, $I$ the moment of inertia of the faceplate beam section, and $E$ the elastic Young's Modulus of the faceplate. Figure 2 shows the models in his calculation, and Fig. 3 plots these deflections or influence functions.

However, the previous FE analyses [4-8] showed that the influence functions (IFs) were Gaussian and extended beyond the actuator by two to three times the actuator spacing for a mirror that was very stiff compared to the actuators and that the influence functions became narrower and less Gaussian in shape as the actuator stiffness increased. The analyses also showed that, for an infinitely stiff actuator, the displacements at neighboring actuators were zero, but the IF changed sign beyond the

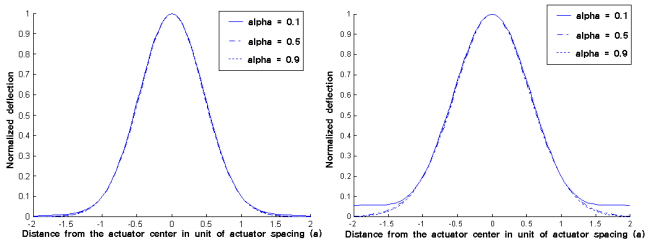


Fig. 3. Normalized influence functions from the derived equation, Eq. (7).

first neighboring actuator, giving rise to a sinc-shaped influence function.

Incorporating the previous FE analyses, the influence functions can generally be modeled as Gaussian functions for a deformable mirror with an infinitely stiff faceplate and as a Gaussian function multiplied by a sinc function for a deformable mirror with an infinitely stiff actuator as follows:

$$y_1 = A\exp\left[-B\left(\frac{x}{a}\right)^2\right], \tag{3}$$

$$y_2 = C\,\mathrm{sinc}\left(\frac{x}{a}\right)\exp\left[-D\left(\frac{x}{a}\right)^2\right], \tag{4}$$

where $A$, $B$, $C$, and $D$ are constants that depend on the mechanical properties and the geometries of the mirror and the actuators.

### 2. Influence Functions of Real Deformable Mirrors

Since real deformable mirrors are between those the two ideal cases discussed above, the deflections or influence functions of real deformable mirrors can be assumed to be linear combinations of those two ideal cases:

$$y = \alpha y_1 + (1-\alpha)y_2, \tag{5}$$

where $y$ is the deflection of a real deformable mirror. In this equation, the condition $\alpha = 0$ represents an infinitely stiff actuator. At the other extreme, the condition $\alpha = 1$ corresponds to an infinitely stiff faceplate.

Here, we define the coupling constant $C_A$ as the ratio of the faceplate deflection at an adjacent actuator to that of the peak deflection due to an energized actuator:

$$C_A = \frac{y(a)}{y(0)} = \frac{\alpha A\exp(-B)}{\alpha A + (1-\alpha)C}, \tag{6}$$

In addition, since Hardy's derivation is still a valid approximation around a central actuator, *i.e.*, $x << a$, the relation $A = 4C$ is true. Furthermore, since the constants $B$ and $D$ are shown to be dominantly determined by the actuator space $a$ [4-11], we can set $B = D$ without losing much calculation accuracy.

Therefore, from the previous relations, we can rewrite the deflection as a function of the coupling constant $C_A$ and $\alpha$ as follows:

$$y = C_1 \left(4\alpha + (1-\alpha)\mathrm{sinc}\left(\frac{x}{a}\right)\right) \times \exp\left[ln\left(C_A \frac{1+3\alpha}{4\alpha}\right)\left(\frac{x}{a}\right)^2\right], \quad (7)$$

with $C_1 = \frac{a^3 F}{24EI}$. Figure 3 plots the normalized deflections or influence functions for $\alpha = 0.1$, 0.5, and 0.9 with $C_A = 0.1$ and $C_A = 0.2$. This figure shows that the overall shapes of the influence functions are practically identical within one actuator spacing and differ beyond one actuator spacing $a$ when $C_A > 0.15$. Since most manufactured deformable mirrors have coupling constants, $C_A$, less than 0.1, practical influence functions can be formulated as Gaussians, which are only functions of the coupling constant $C_A$, the actuator spacing $a$, and the mechanical properties.

## III. PERFORMANCE ANALYSIS

### 1. Mathematical Framework

The performance analysis assumed perfect and instant wavefront sensing and instant wavefront correction, which means the analysis was performed primarily for estimating the fitting errors of the deformable mirrors. For an incoming wavefront distortion $\phi(r,\theta)$ over a circular aperture of arbitrary radius R, the deformable mirror (DM) generates its approximate conjugate $\hat{\phi}(r,\theta)$ in order to minimize the residual fitting error $e^2$ as given by

$$\hat{\phi}(R\rho,\theta) = \sum_{i=1}^{m} a_i r_i(\rho,\theta), \quad (8)$$

$$e^2 = \int\int \left[\rho - \hat{\rho}\right]^2 W(\rho)\rho d\rho d\theta, \quad (9)$$

where $\rho = r/R$, $a_i$ is the command to the $i^{th}$ actuator, $r_i$ is the influence function of the $i^{th}$ actuator, and the aperture function $W(\rho) = 1/\pi$ only when $\rho \leq 1$.

Suppose we sample the DM surface at $n$ surface points $\boldsymbol{x}_j$, j=1,. . .,n, with a normalized sampling distance $S = \Delta x/R$; then, the relationship between the surface position and the actuator command can be described in matrix notation as $\hat{\phi} = Ha$, where the $n$ dimensional vector $\hat{\phi} = \left[\hat{\phi}(\boldsymbol{x}_1), \ldots, \hat{\phi}(\boldsymbol{x}_n)\right]^T$ represents the discrete corrected phase profile and the $n \times m$ DM configuration matrix $H$ has the $i^{th}$ column vector $[r_i(\boldsymbol{x}_1), \ldots, r_i(\boldsymbol{x}_n)]^T$. Then, the actuator control signal $a_i(t)$ and the residual error $e^2$ become

$$a(t) = (H^T H)^{-1} H^T \phi(t), \quad (10)$$

$$e^2 = \frac{1}{\pi} S^2 \phi^T P \phi, \quad (11)$$

$$P = \left[I - H(H^T H)^{-1} H^T\right]^T \left[I - H(H^T H)^{-1} H^T\right], \quad (12)$$

where $I$ is the identity matrix.

When the phase is decomposed by Zernike polynomials $Z_i$ as $\phi = \sum a_i Z_i$, the fitting error in Eq. (11) can be rewritten as

$$e^2 = \frac{1}{\pi} S^2 \sum_i \sum_j a_i a_j Z_i^T P Z_j, \quad (13)$$

For an ensemble-averaged fitting error for atmospheric distortion, Eq. (13) is given with the atmospheric distortion's covariance matrix $C_{ij} =< a_i a_j >$, which was derived by Roddier [11]:

$$< e^2 >= \frac{1}{\pi} S^2 \sum_i \sum_j C_{ij} Z_i^T P Z_j, \quad (14)$$

The nominal Zernike polynomial wavefront fitting error in Eq. (13) becomes zero for a perfect match and one for a perfect non-match. Therefore, if we define the fitting ability $FA_i$ for the $i^{th}$ Zernike polynomial by following Noll's definition [9], $FA_i$ becomes one for a perfect match for the $i^{th}$ Zernike polynomial and zero for a perfect non-match. This fitting ability $FA_i$ describes how well the mirror matches the Zernike polynomials:

$$FA_i = 1 - \frac{1}{\pi} S^2 Z_i^T P Z_i, \quad (15)$$

### 2. Deformable Mirror Models

The fitting errors are calculated for three topologies: hexagonal, square, and triangular. These three topologies provide point support grids that are identical for all support points. Fgiure 4 shows the number of actuators and layout of the first four layouts of each topology.

### 3. Analysis Results

The first analysis is performed to see how the actuator coupling ($0 < C_A < 0.3$) and the linear combination ratio ($0 < \alpha < 1$) affect the overall fitting ability. Figure 5 shows the ensemble-averaged fitting errors of two triangular layouts (19 and 37 actuators) for atmospheric distortion.

From Fig. 5, it is clear that the overall performance of 37 actuators is better than that of 19 actuators. Adding to that, the following conclusions can be reached: 1) the overall performance is quite constant except for an area $C_A \approx 0$ and $\alpha \approx 1$; 2) when $\alpha \approx 0$, *i.e.*, when the actuator provides free local tip/tilt of deformable mirrors as designed in another paper [6] using flexures, the fitting

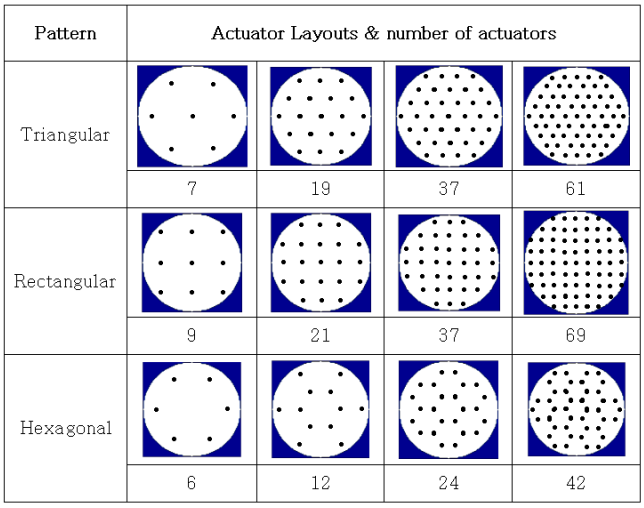


Fig. 4. The number of actuators and actuator layouts.

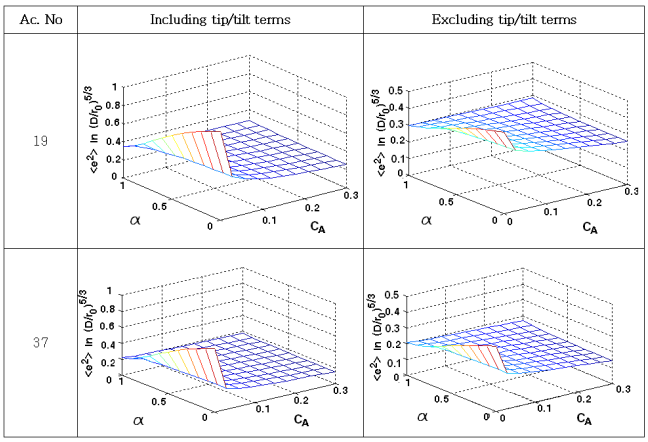


Fig. 5. Ensemble-averaged fitting errors of the triangular layouts (19 and 37 actuators) for atmospheric distortion.

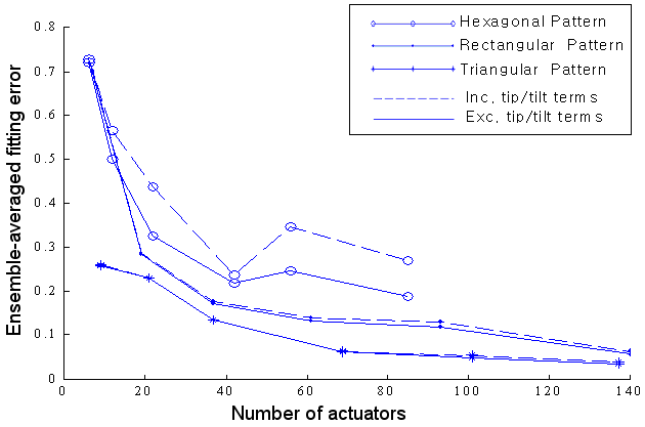


Fig. 6. Ensemble-averaged fitting errors for atmospheric distortion.

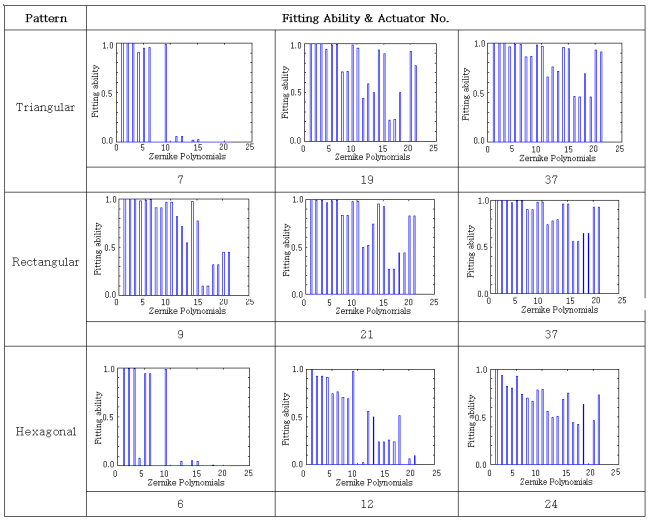


Fig. 7. Fitting ability of the first three layouts of each topology.

ability is stable regardless of the value of $C_A$; 3) when $\alpha \approx 1$, *i.e.*, when the actuator does not provide any free local tip/tilt of deformable mirrors, $C_A$ should be larger than $0.1 \sim 0.2$.

In the previous section, the overall performance was shown to be quite constant except for an area $C_A \approx 0$ and $\alpha \approx 1$. Therefore, $C_A = 0.2$ and $\alpha = 0.1$, selected because they are the results of the FE analysis and the preliminary test of a deformable mirror [6,7], are used for analyzing the fitting ability of deformable mirrors with three topologies. Figure 6 shows the change of the ensemble fitting error for atmospheric distortions as the number of actuators is increased. In this figure, the fitting ability of the triangular pattern is the best of the three topologies. From this figure, the minimum required number of actuators can be derived for given residual errors. However, there is no significant improvement in fitting ability over 70 actuators. Figure 7 shows how well each pattern matches each Zernike polynomial. If the deformable mirror is to correct specific orders of Zernike polynomials, the table in Fig. 7 might guide the selection.

## IV. CONCLUSIONS

This paper derives mathematical IF equations based on simple beam theory and FEA calculations. From those equations, the fitting ability of the deformable mirrors were analyzed, showing that the overall performance is basically constant regardless of coupling constant $C_A$ and the linear combination ratio $\alpha$ except when $C_A \approx 0$ and $\alpha \approx 1$.

Using the values of $C_A$ and $\alpha$, selected since they are the results of the FEM analysis and preliminary test of a deformable mirror, the ensemble fitting errors are calculated for three topologies, finding the order of fitting ability of three patterns: the triangular pattern, rectangular pattern, and hexagonal pattern. Adding to that, it

is found that the deformable mirror does not show significant improvement over the actuator number of about 70.

Based on this study, further study will be carried out to determine the optimum layout of actuators for given wavefront distortions using a minimum number of actuators. This study also can be applied in the optimization of deformable mirrors which aim to compensate specific aberrations such as spherical and defocus aberrations issued in inflatable membrane mirrors [12].

## ACKNOWLEDGMENTS

The authors are grateful to the Satellite Technology Research Center (SaTReC), Korea Advanced Institute of Science and Technology (KAIST) for sponsoring the present research.

## REFERENCES

[1] J. M. Beckers, Ann. Rev. Astronomy and Astrophysics **31**, 13 (1993).
[2] Seung-Kyu Park, Sung-Hoon Baik, Young-Seok Seo, Cheol-Jung Kim and S. W. Ra, J. Korean Phys. Soc. **42**, 743 (2003).
[3] J. W. Hardy, *Adaptive Optics for Astronomical Telescopes* (Oxford University Press, New York, 1998).
[4] R. H. Hudgin, J. Opt. Soc. Am. **67**, 393 (1977).
[5] V. G. Taranenko, G. P. Koshelev and N. S. Romanyuk, Sov. J. Opt. Technol. **48**, 650 (1981).
[6] J. H. Lee, D. D. Walker and A.P. Doel, Opt. Eng. **38**, 1456 (1999).
[7] J. H. Lee, D. D. Walker and A.P. Doel, Opt. Eng. **39**, 1057 (2000).
[8] R. K. Tyson, *Principles of Adaptive Optics* (Academic Press, 1991).
[9] R. J. Noll, J. Opt. Soc. Am **66**, 207 (1976).
[10] M. Y. Chu, V.P. Pauca, R. J. Plemmons and X. Sun, Linear Algebra and Its Applications **316**, 113 (2000).
[11] N. Roddier, Proc. SPIE **1237**, 558 (1990).
[12] M. Soh, J. H. Lee and S. Youn, J. Korean Phys. Soc. **44**, 854 (2004).